Dynamics of microcavity polaritons in the presence of an electron gas

D. Bajoni,[1,*] M. Perrin,[1] P. Senellart,[1] A. Lemaître,[1] B. Sermage,[2] and J. Bloch[1]
[1]*Laboratoire de Photonique et de Nanostructures, Route de Nozay, 91460 Marcoussis, France*
[2]*France Telecom Div. R&D, 38-40 rue du Général Leclerc, 92794 Issy-les-Moulineaux Cedex, France*
(Received 30 November 2005; published 24 May 2006)

The dynamics of microcavity polaritons in the presence of an electron gas is experimentally studied through time-resolved photoluminescence under nonresonant excitation. Electrons are shown to accelerate the emission dynamics of the whole system, both in the polariton trap close to the center of the Brillouin zone ($k=0$) and in the reservoir of large in-plane wave-vector excitonic states. By studying both the bare quantum well and the microcavity sample, the observed features are explained by the interplay between the physics of excitons and that of polariton relaxation.

DOI: 10.1103/PhysRevB.73.205344 PACS number(s): 71.36.+c, 71.35.Pq, 78.47.+p

I. INTRODUCTION

Microcavity polaritons are mixed exciton-photon states, arising from the strong coupling of quantum well (QW) excitons and the optical mode of a high-finesse microcavity.[1,2] Their dispersion in k space resembles that of the excitons for high in-plane wave vectors k, but the lower polariton branch shows a trap at the origin. For this reason they have attracted attention as candidates for the observation of quantum statistical effects on the polariton gas.[3–7]

In a typical nonresonant photoluminescence (PL) experiment, a high-energy laser beam is used to inject electron-hole pairs in the system, resulting in the formation of high-energy, high-wave-vector excitons. The excitons then relax toward lower energies down to the polariton branch, mainly by emission of phonons. However, polariton states in the trap have a strongly photonic nature, which results in radiative lifetimes shrinking below the acoustic phonon-polariton scattering times. Therefore polaritons accumulate in the high-k states at the edge of the trap (reservoir states) (Ref. 8) and a relaxation bottleneck is experimentally found.[9–11] With increasing pumping power, polariton-polariton scattering becomes a significative relaxation mechanism between the reservoir and the $k=0$ states. Occupation factors larger than unity have indeed been observed in II-VI-based microcavities.[12–14] On the contrary, in GaAs-based systems, the loss of the strong-coupling regime due to exciton broadening occurs before the polariton-polariton scattering rate overcomes radiative losses.[15,16]

Electron-polariton scattering has been recently proposed as an efficient relaxation mechanism to reach polariton thermalization and possibly condensation.[17] Indeed electron-polariton collisions have a high cross section: electrons have a steeper dispersion than acoustic phonons, and thus fewer collisions are needed in order to reach the polariton band minimum; moreover, electron-polariton scattering should be more efficient than polariton-polariton scattering because the monopole-dipole interaction is stronger than the dipole-dipole interaction.

The strong-coupling regime with both the exciton and trion have been reported in a microcavity containing an electron gas.[18] Continuous-wave luminescence has shown an increased population of the $k=0$ states[19,20] and improved thermalization of polaritons in the polariton trap as the electron gas is injected.[21]

In the present paper we study the effects of a photoinjected electron gas on the dynamics of microcavity polaritons by means of time-resolved PL under nonresonant pulsed excitation. To help to get an overall understanding of these results we first consider the dynamics of a reference sample consisting of a bare QW. This allows us to distinguish the modifications induced by the electron gas related to the physics of excitons from the features related to the physics of microcavities in the strong-coupling regime. The electron gas is shown to strongly accelerate the QW emission dynamics both because of a faster exciton formation and because of an equilibrium with a trion population. Then we investigate the dynamics of the polariton states at the bottom of the polariton trap and at large in-plane wave vectors (excitoniclike reservoir). The dynamics of the reservoir is found to be exactly the same as the reference QW. We show that the population at $k=0$ follows the instantaneous population of the reservoir. As a consequence the dynamics at $k=0$ is twice faster than the reservoir if the main relaxation mechanism is polariton-polariton scattering and is similar to the reservoir dynamics when electron-polariton scattering dominates. Depending on the excitation conditions, the relative strength of the two scattering mechanisms can be controlled.

The paper is organized as follows: in Sec. II, we describe the sample structure and the experimental setup. In Sec. III, we analyze the dynamics of the excitons not coupled to a cavity mode. We study in Sec. IV the time-resolved measurements obtained on the microcavity sample. We numerically simulate the PL decay curve in Sec. V and conclude in Sec. VI.

II. SAMPLE AND EXPERIMENTAL SETUP

The sample is a $\lambda/2$ AlAs cavity with a top (bottom) Bragg mirror of 15 (25) $Al_{0.1}Ga_{0.9}As/AlAs$ pairs on a GaAs substrate. A mixed-type QW structure is placed at the antinode of the cavity mode:[22] it contains a wide GaAs QW (20 nm), surrounded by two narrow GaAs QW's (2.6 nm). The narrow QW's are separated from the wide QW by AlAs barriers (10 nm). When the narrow QW's are photoexcited

by a high-energy laser beam, the generated electrons quickly transfer toward the lower energy levels of the large QW through the X valley of the AlAs barrier (with transfer time in the ps range[23]). On the other hand, holes can transfer to the wide QW only by tunneling through the barrier with a transfer time many orders of magnitude longer (in the ms range[24]). An electron gas is thus formed in the large QW, the density of which is optically controlled.

The heavy-hole and light-hole excitons of the wide QW are in strong coupling with the cavity mode: the Rabi splitting is 4.4 meV for the heavy-hole exciton and 3.2 meV for the light-hole exciton. The cavity is wedge shaped, so that the difference in energy between the cavity mode and the QW exciton at $k=0$ (detuning Δ) may be tuned by changing the investigated spot on the sample.

In our experiment, the sample is kept at 12 K. Excitons are nonresonantly injected in the wide QW with a mode-locked Ti:sapphire laser delivering 1.5-ps pulses, which is tuned to an energy 120 meV above the heavy-hole exciton transition. A He:Ne laser is used to create the electron gas. Both beams are focused onto the same spot (~ 30 μm diameter) on the sample surface. A diaphragm allows an angular selection of the PL signal with an angular resolution of $\sim 2°$. The detection angle θ is directly linked to the in-plane wave vector k of the emitting states through the relation $k=(\omega/c)\sin\theta$, ω being the frequency of the emitted radiation. The signal is then spectrally dispersed and temporally analyzed by a Syncroscan streak camera. The spectral resolution is ~ 0.3 meV, while the temporal resolution is ~ 35 ps.

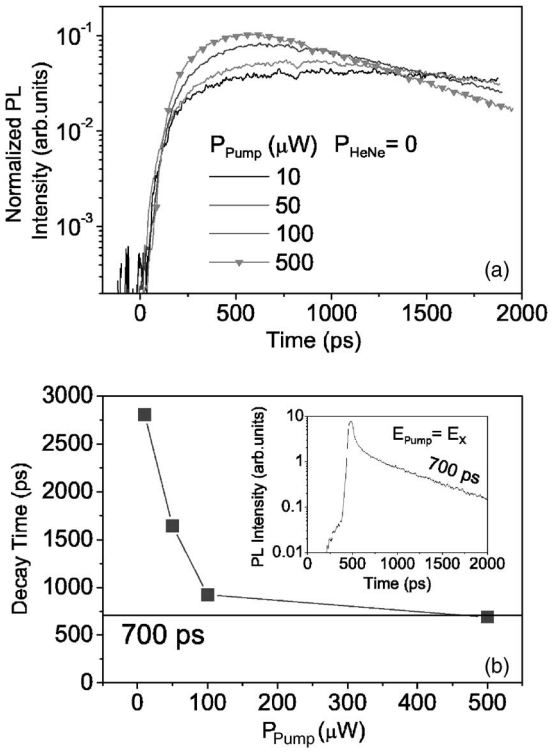

FIG. 1. (a) Time-resolved exciton PL intensity, for increasing excitation powers in the absence of the electron gas, under nonresonant excitation. The curves are normalized to P_{pump}. (b) Decay times as a function of the excitation power extracted from the curves of (a). Inset: time-resolved exciton PL intensity, with the excitation energy at resonance with the exciton line.

III. DYNAMICS OF THE EXCITONS IN THE BARE QW

In order to understand the dynamics of microcavity polaritons, we first study the emission dynamics of excitons not coupled to a cavity mode. To do so, the upper mirror of our cavity sample was removed by chemical etching.

We consider exciton emission dynamics in the absence of electrons. Figure 1(a) shows the heavy-hole exciton emission as a function of time for increasing excitation powers (P_{pump}): the decay curves are normalized to the pump power. At low powers, the system exhibits a slow dynamic, with both long rise and decay times. With increasing P_{pump} both times become shorter. The measured decay times (τ_{dec}) are plotted in Fig. 1(b): τ_{dec} goes from 3 ns at low P_{pump} down to a saturation value of 700 ps at higher power.

As shown by Szczytko *et al.*,[25] at low P_{pump}, the exciton bimolecular formation is slow and limits the emission dynamics. This is why decay times as long as several nanoseconds can be measured. Since the bimolecular exciton formation process is proportional to the square of the free-carrier density, it quadratically increases with P_{pump}. Thus, at high excitation powers, the exciton formation becomes a fast process. Since the exciton cooling time is of the order of 100 ps,[26] the exciton distribution does not evolve anymore for longer time delays. As a consequence the 700-ps PL decay time corresponds to the average radiative lifetime of thermalized excitons.[27–29] To check this interpretation, the decay time of thermalized excitons has been directly measured by performing time-resolved PL under excitation resonant to the exciton line.[30–32] In this configuration the resonantly injected excitons quickly redistribute along the dispersion curve by interaction with the phonon bath: the measured decay time is then the mean radiative lifetime of a thermalized exciton population consisting of optically active ($k<3\times10^5$ cm^{-1}) and non-optically-active excitons ($k>3\times10^5$ cm^{-1}).[27,28] The measured decay curve under resonant excitation is shown in the inset of Fig. 1(b) and indeed evidences a 700-ps decay time.

Let us now consider the modification of the QW emission induced by the electron gas. Figure 2(a) shows the time-integrated PL spectra measured with a constant pump power of 50 μW, at several He:Ne powers ($P_{\mathrm{He:Ne}}$). Without electrons, the emission line at 1.528 eV is attributed to the heavy-hole exciton transition. When electrons are injected, a second line appears, 1.4 meV below the heavy-hole exciton. This line is related to negatively charged excitons or trions.[33,34] With increasing He:Ne power, the exciton line loses intensity, while the trion line becomes stronger, eventually dominating the PL spectrum.[35,36]

In our measurements, trions and excitons present the same temporal behavior, indicating a thermal equilibrium at all time delays between the two species.[35] The decay curves presented in Fig. 2(b) [which correspond to the spectra shown in Fig. 2(a)] result from a spectral integration over both the exciton and trion lines. In this figure, the exciton dynamics is slow in the absence of electrons being limited by

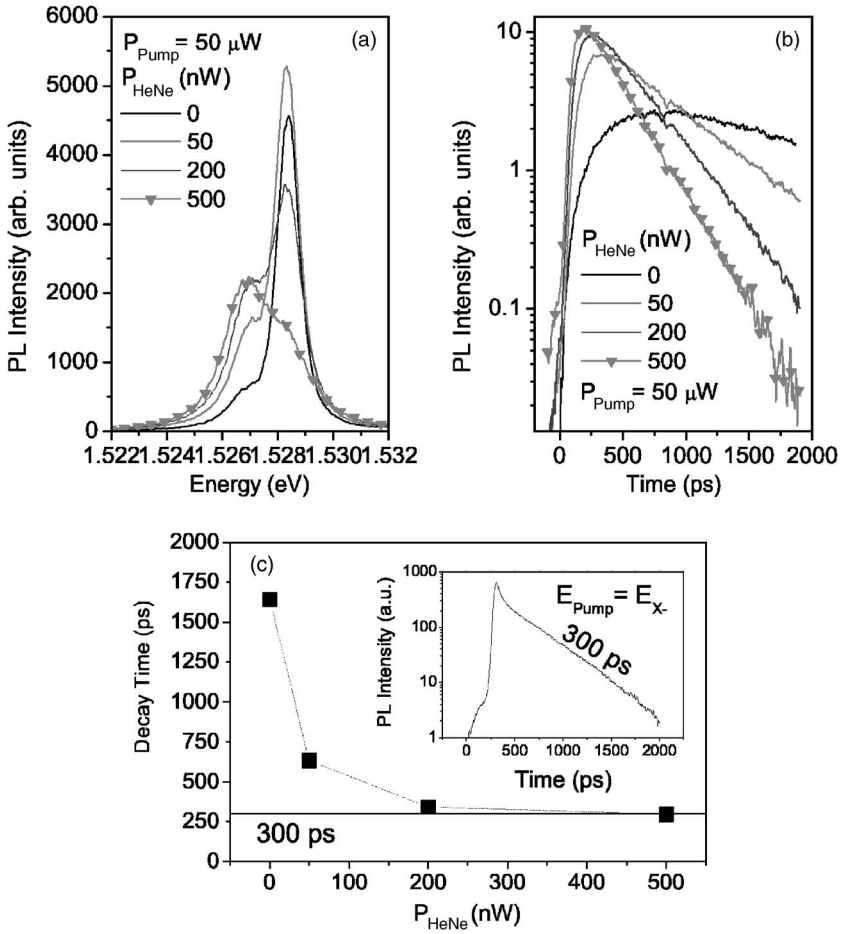

FIG. 2. (a) Time-integrated PL spectra and (b) time-resolved exciton PL intensity, for increasing He:Ne powers, under nonresonant excitation. (c): Decay times as a function of the He:Ne power extracted from the curves of (b). Inset: time-resolved trion PL intensity, with the excitation energy at resonance with the trion line and the He:Ne power set at 1 μW.

the exciton formation. When injecting electrons, the excess of carriers accelerates the exciton formation and both rise and decay times get progressively shorter. The measured decay times are summarized in Fig. 2(c) as a function of the HeNe power: the emission decay time is reduced down to a saturation value of 300 ps at the highest investigated He:Ne power. This value corresponds to the trion decay time: this has been confirmed by resonantly exciting the trion transition[32,37] under a 1-μW He:Ne excitation power. The corresponding decay curve is shown in the inset of Fig. 2(c): the measured decay time, which directly reflects the trion mean radiative lifetime, amounts indeed to 300 ps. Notice that for this temperature, the exciton radiative lifetime (700 ps) is longer than the trion radiative lifetime (300 ps). Finally let us underline that under nonresonant excitation when adding electrons the PL decay time goes down to 300 ps before the complete disappearance of the exciton line in the emission spectrum. This behavior is at present not clearly understood.

To conclude these measurements show that in the absence of a cavity effect, the exciton dynamics strongly depends both on the exciton density and on the electron density.

IV. DYNAMICS OF POLARITONS

We now consider the dynamics of the microcavity structure in the strong-coupling regime. Notice that in this structure, the He:Ne beam undergoes 20-dB losses before reaching the QW, due to absorption from AlGaAs in the upper Bragg mirror. Thus a He:Ne power of 40 μW on the microcavity sample corresponds to ~400 nW in the experiment without the top mirror.

Time-resolved spectroscopy has been performed at strong negative detuning ($\Delta=-8$ meV). The measured dispersion curve is shown in Fig. 3; it was obtained by extracting the energy of the two emission peaks (upper and lower polaritons) in the PL spectra for various detection angles.

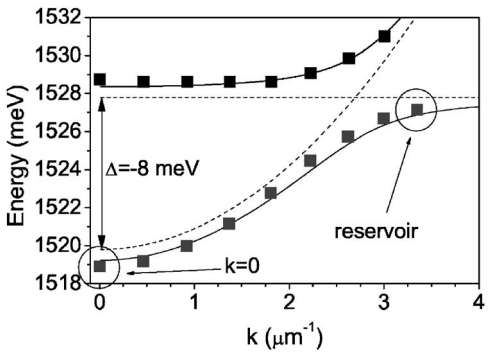

FIG. 3. Measured (symbols) and simulated (solid lines) dispersion curve for $\Delta=-8$ meV. The two investigated states ($k=0$ and reservoir) are highlighted with circles. The dashed lines represent the energy of the uncoupled exciton and cavity modes.

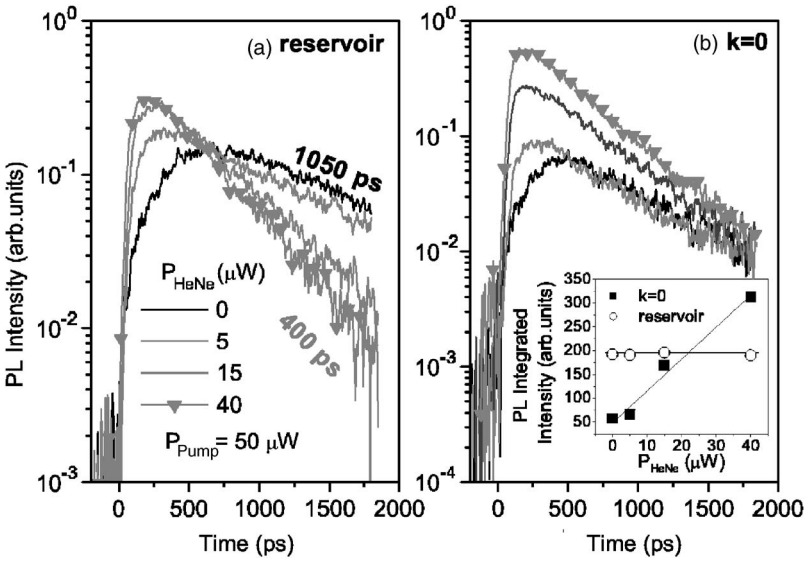

FIG. 4. PL intensity as a function of time for (a) the reservoir and (b) $k=0$ states for increasing powers of the He:Ne beam. Inset: integrated PL intensities for the reservoir (open circles) and $k=0$ states (black squares) as a function of the He:Ne power.

We investigate the dynamics of two particular sets of polariton states. The first one corresponds to polariton states close to $k=0$ in the bottom of the polariton trap. The second set corresponds to excitoniclike states of the reservoir close to $k=3.5\ \mu\mathrm{m}^{-1}$.

The inset of Fig. 4 summarizes the time-integrated PL intensities both at $k=0$ and in the reservoir. As was reported for cw excitation,[21] the PL intensity of the reservoir states is not affected by the electron injection: this proves that in the investigated density range, electrons do not introduce nonradiative decay processes (Auger process) for the polariton population. A significant increase in the integrated PL signal is observed at $k=0$ as electrons are injected. The emission intensity at $k=0$ is enhanced by a factor of ~ 6 at the highest He:Ne power: electron-polariton scattering provides an additional mechanism to relax from the reservoir down to the polariton trap.[17] As a result, in the presence of the electron gas an increased number of polaritons transfer toward the trap and the bottleneck amplitude is reduced.[21] As we discussed in Ref. 21, a strong increase of the population at $k=0$ can be observed without any significant change of the population of each reservoir state: this is explained by the huge density of states of the reservoir as compared to the density of states in the polariton trap.

Figures 4(a) and 4(b) show the time-resolved PL both in the reservoir and at $k=0$ for increasing He:Ne powers. The reservoir decay curves show the same qualitative evolution with increasing electron densities as described in Sec. III for the reference sample. The decay time (τ_{dec}^{res}) decreases continuously as the He:Ne power increases. In these measurements, the saturation value of τ_{dec}^{res} amounts to 400 ps. So the trion lifetime in the cavity sample is found to be slightly larger in value than the 300 ps found in the bare QW. This can be attributed to a small increase of the sample temperature induced by the absorption of the He:Ne beam in the top mirror.[28] Since we have to use a He:Ne power 100 times stronger in the cavity sample than in the bare quantum well to inject the same electron density, heating is much more important in the cavity sample.

In the case of $k=0$ states, we also observe an acceleration of the emission dynamics as electrons are injected in the system. This acceleration seems qualitatively similar to that of the reservoir states.

To complete our analysis of electron-polariton scattering and compare it to polariton-polariton scattering, we now address the influence of the Ti:sapphire power on the emission dynamics. Figure 5(a) [Fig. 5(d)] shows the decay curves measured at $k=0$ and in the reservoir in the absence [in the presence] of electrons for several Ti:sapphire excitation powers. The curves have been vertically shifted in order to make the $k=0$ and reservoir maximum intensity coincide at each excitation power.

It can be seen in Figs. 5(a) and 5(d), that the reservoir dynamics varies exactly as in the uncoupled QW when increasing the Ti:sapphire power or when injecting an electron gas. In the absence of electrons [Fig. 5(a)], both the rise and decay times of the reservoir get shorter with increasing pumping rates due to a faster exciton formation [see Fig. 5(b)]. The decay time saturates at 700 ps, the radiative lifetime of thermalized excitons in the reservoir. When the electron gas is added to the system, the reservoir dynamics is accelerated and remains unchanged for all excitation powers with a decay time of the order of 400 ps [Fig. 5(e)], characteristic of a strongly-trion-like state. The fact that the physics of the reservoir states is identical to that of the uncoupled excitons is of course due to the strong excitonic nature of these states. However, it also means that the improved scattering toward the $k=0$ states observed in the presence of electrons (reflected by the increased signal at $k=0$) does not reduce in a detectable way the decay time of the reservoir states.

Before analyzing the emission dynamics at $k=0$, we discuss rate equations which describe the evolution of the system. We demonstrate that the $k=0$ population instantaneously follows that of the reservoir. This allows understanding the overall dynamics at $k=0$ in the different excitation conditions.

The system is divided into three subsystems: the injected electrons and holes, the reservoir, and the $k=0$ states. The time evolution of the different populations is written as follows:

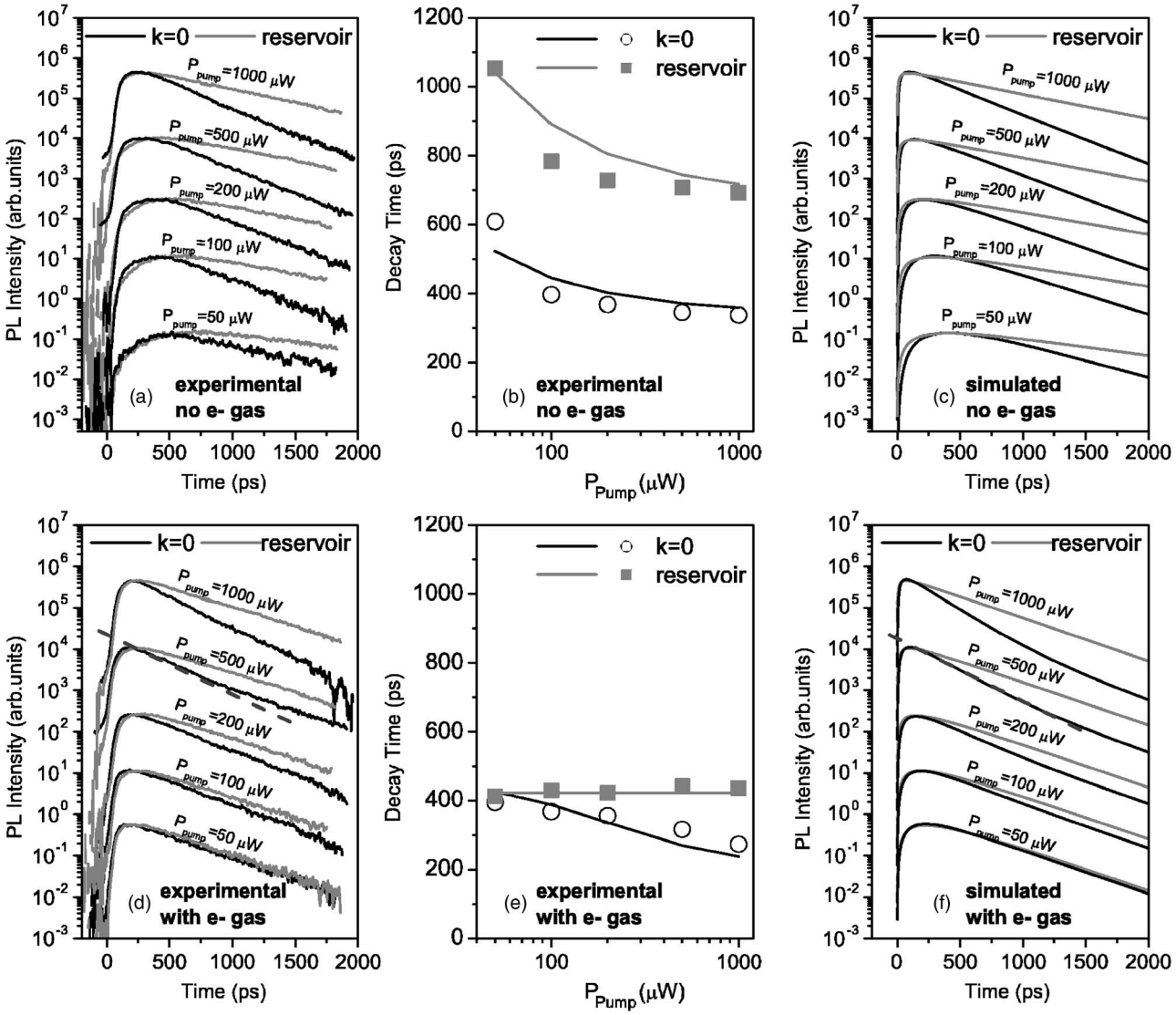

FIG. 5. (a) PL intensity measured as a function of time for $k=0$ (black lines) and in the reservoir (gray lines) for $P_{\mathrm{He:Ne}}=0$. (b) Decay times for the $k=0$ states (black open circles) and for the reservoir (gray squares) extracted from the decay curves of (a); solid lines correspond to the decay times extracted from the simulated curves of (c). (c) Simulated decay curves corresponding to panel (a). (d) PL intensity measured as a function of time for $k=0$ (black lines) and for the reservoir (gray lines) for $P_{\mathrm{He:Ne}}=40$ μW. (e) Initial decay times for $k=0$ (black open circles) and decay time of the reservoir (gray squares) extracted from the decay curves of (d); solid lines correspond to the decay times extracted from the simulated curves of (f). (f) Simulated decay curves corresponding to panel (d). In panels (a), (c), (d), and (f) the decay curves have been vertically shifted so that the $k=0$ and reservoir maximum intensity coincide at each excitation power. In panels (d) and (f), the dashed line highlights the $k=0$ initial decay for $P_{pump}=500$ μW. Panels (c) and (f) will be discussed in Sec. V.

$$\frac{dn_e(t)}{dt} = n^0 \cdot \delta(t) - C \cdot n_e(t) n_h(t), \tag{1a}$$

$$\frac{dn_h(t)}{dt} = n^0 \cdot \delta(t) - C \cdot n_e(t) n_h(t), \tag{1b}$$

$$\frac{dn_{res}(t)}{dt} = C \cdot n_e(t) n_h(t) - \frac{n_{res}(t)}{\tau_{res}} - W_{pol\text{-}pol} \cdot n_{res}(t)^2 - W_{el\text{-}pol} \cdot n_e(t) n_{res}(t), \tag{1c}$$

$$\frac{dn_{k=0}(t)}{dt} = -\frac{n_{k=0}(t)\alpha_{k=0}}{\tau_C} + W_{pol\text{-}pol} \cdot n_{res}(t)^2 + W_{el\text{-}pol} \cdot n_e(t) n_{res}(t). \tag{1d}$$

Here C is the bimolecular exciton formation rate from the plasma and $\delta(t)$ is the Dirac function. n^0 is the initial number of electron-hole pairs injected by the pump while $n_e(t)$ and $n_h(t)$ are the time-dependent populations for, respectively, the electrons and holes in the plasma. $n_{k=0}(t)$ and $n_{res}(t)$ are the populations of polaritons at $k=0$ and in the reservoir. An additional number of electrons, n_e^0, constant over time, is added to $n_e(t)$ when considering the dynamics under He:Ne

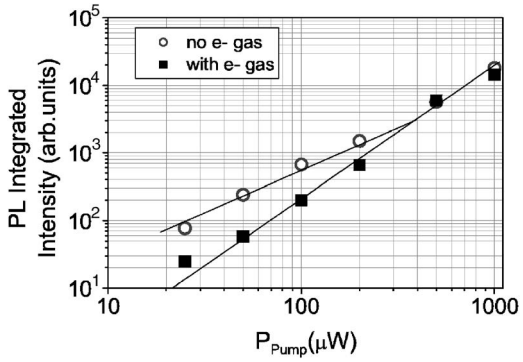

FIG. 6. Integrated PL intensities of the $k=0$ states as a function of the pump power without electrons (solid squares) and with electrons (open circles). The solid lines are guides to the eye.

pumping. $\alpha_{k=0}\sim 0.94$ is the photon fraction for the $k=0$ states. τ_{res} is the radiative lifetime of the reservoir, and $\tau_C=2.2$ ps is the lifetime of the cavity mode (estimated from the polariton linewidth at large negative Δ). $W_{pol\text{-}pol}\cdot n_{res}(t)$ and $W_{el\text{-}pol}\cdot n_e(t)$ are the scattering rates from the reservoir toward the $k=0$ states for, respectively, polariton-polariton and electron-polariton scattering. Notice that in Eqs. (1) the injected plasma may only decay via exciton formation: this is justified by the fact that the bimolecular radiative recombination rate is negligible with respect to the exciton formation rate.[38]

Equation (1d) can be formally integrated as

$$n_{k=0}(t)=\int_0^t e^{-(t-t')/\tau_{k=0}}\left[W_{pol\text{-}pol}\cdot n_{res}(t')^2 + W_{el\text{-}pol}\cdot n_e(t')n_{res}(t')\right]dt', \tag{2}$$

where $\tau_{k=0}=\alpha_{k=0}/\tau_C=2.3$ ps is the radiative lifetime of $k=0$ polaritons. Because of the exponential in Eq. (2), terms with t' such that $t-t'\gg\tau_{k=0}$ do not contribute to the integral. Then, considering that $n_{res}(t)$ and $n_e(t)$ slowly vary on the time scale of $\tau_{k=0}$, we can derive

$$n_{k=0}(t)\approx\left[W_{pol\text{-}pol}\cdot n_{res}(t)^2+W_{el\text{-}pol}\cdot n_e(t)n_{res}(t)\right]\times\int_0^t e^{-(t-t')/\tau_{k=0}}dt' \tag{3}$$

and thus

$$n_{k=0}(t)\approx\left[W_{pol\text{-}pol}\cdot n_{res}(t)^2+W_{el\text{-}pol}\cdot n_e(t)n_{res}(t)\right]\tau_{k=0}. \tag{4}$$

Equation (4) shows that the population at $k=0$ instantaneously follows that of the reservoir.[8,39] Thus, if the reservoir exponentially decays with a decay time τ_{dec}^{res}, $n_{k=0}$ decays with a time constant equal to $\tau_{dec}^{res}/2$ if polariton-polariton scattering is dominant and to τ_{dec}^{res} if electron-polariton rate scattering is the largest.

Let us now consider the emission measured at $k=0$, at first in the absence of electrons. The integrated PL intensity of the emission at $k=0$ is reported in Fig. 6; when increasing the excitation power, the signal at $k=0$ grows quadratically, a signature of polariton-polariton scattering.[40] As a consequence, the decay time $\tau_{dec}^{k=0}$ of $k=0$ states is equal to one-half of the reservoir decay time τ_{dec}^{res} [see Fig. 5(b)]. When increasing the excitation power, the dynamics in the reservoir continuously accelerates because of a faster exciton formation and its decay time goes down to 700 ps. Consequently the decay time at $k=0$ goes down to $\tau_{dec}^{k=0}=700/2=350$ ps: the acceleration of the dynamics observed at $k=0$ simply reflects the faster exciton formation in the reservoir.

Let us now consider the emission at $k=0$ in the presence of the electron gas. The PL intensity at low Ti:sapphire excitation powers (open circles in Fig. 6) is enhanced and grows quasilinearly with the excitation power: electron-polariton interactions now govern the relaxation from the reservoir into the polariton trap. Thus, as derived in Eq. (4), the emission dynamics at $k=0$ is identical to that of the reservoir. Figure 5(e) indeed shows that at low excitation power, $\tau_{dec}^{k=0}$ and τ_{dec}^{res} are equal. Then, when the excitation power is increased, polariton-polariton scattering becomes stronger and eventually dominates the relaxation.[21] As a consequence, the dynamics at $k=0$ progressively becomes faster than that of the reservoir and its decay time tends to half that of the reservoir [see Fig. 5(e)].

Finally, we want to mention that we have investigated the dynamics of our microcavity for several detunings. The physics of the system always remains well described by the behavior outlined by Eq. (4) and discussed thereafter. The reservoir dynamics does not depend on Δ and is modified the same way when adding electrons. When going to less negative detunings, the bottleneck amplitude is reduced and the role of polariton-polariton scattering becomes less important. As a result, the emission at $k=0$ becomes closer to a linear behavior and the dynamics in the presence of electrons resembles more and more that of the reservoir. Actually, for zero detuning we observe the very same dynamics at $k=0$ and in the reservoir for any excitation condition.

V. NUMERICAL CALCULATIONS

To complete our analysis of the polariton dynamics and quantify the interplay of the two scattering mechanisms, we numerically solve Eqs. (1) to simulate the experimental decay curves. We have taken $\tau_{res}=700$ ps in the absence and $\tau_{res}=420$ ps in the presence of the electron gas.

The number of injected pairs has been estimated as follows:

$$n^0=\frac{\gamma_{QW}TP_{pump}}{E_{Pump}\Omega}\simeq 500\cdot P_{pump}(\mu W),$$

where $\gamma_{QW}\sim 2.5\%$ is the absorption of the QW, $T\sim 0.44$ is the transmission of the microcavity upper mirror at E_{pump}, and $\Omega=82$ MHz the pump repetition rate. To determine n_e^0, we have extrapolated to the low-density limit the Fermi energy measurements at high electron density.[41,42] We obtain $n_e^0\simeq 1\times 10^8\times P_{\mathrm{He:Ne}}\ (\mu\mathrm{W})\times S\ (\mathrm{cm}^2)$, where S is the spot area.

As experimentally shown in Sec. IV, the dynamics of the reservoir is not affected by the scattering of polaritons into

the polariton trap: we measure exactly the same behavior as in the sample without the top mirror. So to determine the best parameters in our model, we start by fitting the reservoir dynamics solving only the first three equations of the system (1) and neglecting the scattering toward $k=0$: by doing so the only fitting parameter is C. We find $C \sim 1.6 \times 10^5$ s^{-1}, a value fully consistent with the calculations of Ref. 43. Then the dynamics of $k=0$ states has been fitted with $W_{pol\text{-}pol}=4$ s^{-1} (consistent with the value calculated in Ref. 8) and $W_{el\text{-}pol}=5.5$ s^{-1}.

The calculated decay curves are shown in Figs. 5(c) and 5(f). Decay curves for the reservoir and $k=0$ are superimposed for several polariton densities to allow a straightforward comparison with the experimental data of Figs. 5(a) and 5(d). Moreover, calculated decay times are reported in Figs. 5(b) and 5(e) for comparison with experimental values. There is good agreement between the experimental and simulated curves, and the overall dynamics is well reproduced by the model. First, in the absence of electrons, the bimolecular exciton formation reproduces the progressive acceleration of the reservoir dynamics as the polariton density is increased. In these excitation conditions, the emission at $k=0$ decays twice faster than the reservoir, a signature of the quadratic nature of the relaxation mechanism feeding these states. When electrons are introduced in the system, the emission rise time is reduced because of a faster exciton formation and the emission at $k=0$ has the same dynamics as the reservoir as long as the excitation power is low enough for electron-polariton scattering to govern the relaxation. For higher excitation powers, polariton-polariton scattering dominates the relaxation into the trap and the emission at $k=0$ becomes faster than that of the reservoir.

The transition between the two scattering mechanisms is also visible from the more complex decay shapes observed in the intermediate excitation range. Notice, for instance, in Fig. 5(d), the biexponential behavior of the decay curve measured at $k=0$ (in the presence of electrons) for 500 μW excitation power. At short time delays, the decay is faster than that of the reservoir (this first decay has been highlighted with a dashed line in the figure), a signature of strong polariton-polariton scattering. Then, $\sim$500 ps after the emission peak, the polariton population in the reservoir has sufficiently decayed for electron-polariton scattering to become the dominant relaxation mechanism: as a consequence the emission decay becomes slower and identical to the decay of the reservoir. For this excitation power, the relaxation is governed by polariton-polariton scattering at short time delays and by electron-polariton scattering at long time delays. This biexponential decay is reproduced by the model.

VI. CONCLUSIONS

The effect of a photoinjected electron gas on the dynamics of microcavity polaritons has been studied under nonresonant excitation. As previously reported under cw excitation,[21] a strong increase of the signal at $k=0$ is induced by the injection of the electron gas while the signal in the reservoir remains unchanged. However, as under cw excitation, we do not observe any polariton condensation or a depletion of the reservoir.

Time-resolved measurements show that electrons strongly accelerate the emission dynamics of the reservoir states. This behavior is not specific to the microcavity system since it is also observed in a reference QW not coupled to a cavity. It can be explained by a faster exciton formation and, in the presence of electrons, trionic effects. Moreover, it appears as a clear piece of experimental evidence that the dynamics of the reservoir is not affected by the scattering of polaritons toward $k=0$.

Since the overall scattering rate toward $k=0$ is smaller than the polariton radiative rate at $k=0$, we have also shown that the population in the polariton trap follows instantaneously the population of the reservoir. As a consequence, the dynamics in the polariton trap directly reflects the dynamics of the reservoir. When polariton-polariton scattering governs the relaxation, then the emission at $k=0$ decays twice faster than in the reservoir. When electron-polariton scattering dominates, the dynamics observed at $k=0$ is identical to that of the reservoir.

To conclude, by studying the bare QW and the microcavity sample, we explain the modification of the emission dynamics in the presence of an electron gas by the interplay between the physics of excitons in the reservoir and the physics of the polariton relaxation.

ACKNOWLEDGMENTS

This work was partly supported by the "Région Ile de France" and the "Conseil Général de l'Essonne." We also acknowledge the European Community for funding through the Marie Curie project "Clermont 2" Contract No. MRTN-CT-2003-503677. We thank Paul Voisin for a careful reading of the manuscript.

*Electronic address: daniele.bajoni@lpn.cnrs.fr

[1] C. Weisbuch, M. Nishioka, A. Ishikawa, and Y. Arakawa, Phys. Rev. Lett. **69**, 3314 (1992).

[2] For a review see G. Khitrova, H. M. Gibbs, F. Jahnke, M. Kira, and S. W. Koch, Rev. Mod. Phys. **71**, 1591 (1999).

[3] A. Imamoglu, R. J. Ram, S. Pau, and Y. Yamamoto, Phys. Rev. A **53**, 4250 (1996).

[4] F. Tassone and Y. Yamamoto, Phys. Rev. B **59**, 10830 (1999).

[5] F. P. Laussy, G. Malpuech, A. Kavokin, and P. Bigenwald, Phys. Rev. Lett. **93**, 016402 (2004).

[6] F. M. Marchetti, B. D. Simons, and P. B. Littlewood, Phys. Rev. B **70**, 155327 (2004).

[7] Jonathan Keeling, P. R. Eastham, M. H. Szymanska, and P. B. Littlewood, Phys. Rev. B **72**, 115320 (2005).

[8] F. Tassone, C. Piermarocchi, V. Savona, A. Quattropani, and P. Schwendimann, Phys. Rev. B **56**, 7554 (1997).

[9] P. Senellart, J. Bloch, B. Sermage, and J. Y. Marzin, Phys. Rev. B **62**, R16263 (2000).
[10] A. I. Tartakovskii, M. Emam-Ismail, R. M. Stevenson, M. S. Skolnick, V. N. Astratov, D. M. Whittaker, J. J. Baumberg, and J. S. Roberts, Phys. Rev. B **62**, R2283 (2000).
[11] M. Müller, J. Bleuse, and R. André, Phys. Rev. B **62**, 16886 (2000).
[12] F. Boeuf, R. André, R. Romestain, Le Si Dang, E. Péronne, J. F. Lampin, D. Hulin, and A. Alexandrou, Phys. Rev. B **62**, R2279 (2000).
[13] J. Bloch, B. Sermage, M. Perrin, P. Senellart, R. André, and Le Si Dang, Phys. Rev. B **71**, 155311 (2005).
[14] M. Richard, J. Kasprzak, R. Romestain, R. André, and Le Si Dang, Phys. Rev. Lett. **94**, 187401 (2005).
[15] R. Houdré, J. L. Gibernon, P. Pellandini, R. P. Stanley, U. Oesterle, C. Weisbuch, J. O'Gorman, B. Roycroft, and M. Ilegems, Phys. Rev. B **52**, 7810 (1995).
[16] R. Butté, G. Delalleau, A. I. Tartakovskii, M. S. Skolnick, V. N. Astratov, J. J. Baumberg, G. Malpuech, A. Di Carlo, A. V. Kavokin, and J. S. Roberts, Phys. Rev. B **65**, 205310 (2002).
[17] G. Malpuech, A. Kavokin, A. Di Carlo, and J. J. Baumberg, Phys. Rev. B **65**, 153310 (2002).
[18] R. Rapaport, R. Harel, E. Cohen, Arza Ron, E. Linder, and L. N. Pfeiffer, Phys. Rev. Lett. **84**, 1607 (2000).
[19] P. G. Lagoudakis, M. D. Martin, J. J. Baumberg, A. Qarry, E. Cohen, and L. N. Pfeiffer, Phys. Rev. Lett. **90**, 206401 (2003).
[20] A. Qarry, G. Ramon, R. Rapaport, E. Cohen, Arza Ron, A. Mann, E. Linder, and L. N. Pfeiffer, Phys. Rev. B **67**, 115320 (2003).
[21] M. Perrin, P. Senellart, A. Lemaître, and J. Bloch, Phys. Rev. B **72**, 075340 (2005).
[22] I. Galbraith, P. Dawson, and C. T. Foxon, Phys. Rev. B **45**, 13499 (1992).
[23] J. Feldmann, M. Preis, E. O. Göbel, P. Dawson, C. T. Foxon, and I. Galbraith, Solid State Commun. **83**, 245 (1992).
[24] P. Dawson and M. J. Godfrey, Phys. Rev. B **68**, 115326 (2003).
[25] J. Szczytko, L. Kappei, J. Berney, F. Morier-Genoud, M. T. Portella-Oberli, and B. Deveaud, Phys. Rev. Lett. **93**, 137401 (2004).
[26] C. Piermarocchi, F. Tassone, V. Savona, A. Quattropani, and P. Schwendimann, Phys. Rev. B **53**, 15834 (1996).
[27] L. C. Andreani, Solid State Commun. **77**, 641 (1991).
[28] A. Esser, E. Runge, R. Zimmermann, and W. Langbein, Phys. Rev. B **62**, 8232 (2000).
[29] J. Martinez-Pastor, A. Vinattieri, L. Carraresi, M. Colocci, Ph. Roussignol, and G. Weimann, Phys. Rev. B **47**, 10456 (1993).
[30] B. Deveaud, F. Clérot, N. Roy, K. Satzke, B. Sermage, and D. S. Katzer, Phys. Rev. Lett. **67**, 2355 (1991).
[31] B. Sermage, B. Deveaud, K. Satzke, F. Clérot, C. Dumas, N. Roy, D. S. Katzer, F. Mollot, R. Planel, M. Berz, and J. L. Oudar, Superlattices Microstruct. **13**, 271 (1993).
[32] D. Sanvitto, R. A. Hogg, A. J. Shields, D. M. Whittaker, M. Y. Simmons, D. A. Ritchie, and M. Pepper, Phys. Rev. B **62**, R13294 (2000).
[33] K. Kheng, R. T. Cox, Y. Merle d'Aubigné, F. Bassani, K. Saminadayar, and S. Tatarenko, Phys. Rev. Lett. **71**, 1752 (1993).
[34] A. J. Shields, M. Pepper, D. A. Ritchie, M. Y. Simmons, and G. A. C. Jones, Phys. Rev. B **51**, 18049 (1995).
[35] Arza Ron, H. W. Yoon, M. D. Sturge, A. Manassen, E. Cohen, and L. N. Pfeiffer, Solid State Commun. **97**, 741 (1996).
[36] A. Manassen, E. Cohen, Arza Ron, E. Linder, and L. N. Pfeiffer, Phys. Rev. B **54**, 10609 (1996).
[37] V. Ciulin, P. Kossacki, S. Haacke, J.-D. Ganière, B. Deveaud, A. Esser, M. Kutrowski, and T. Wojtowicz, Phys. Rev. B **62**, R16310 (2000).
[38] T. Matsusue and H. Sakaki, Appl. Phys. Lett. **50**, 1429 (1987).
[39] J. Bloch and J. Y. Marzin, Phys. Rev. B **56**, 2103 (1997).
[40] At this strongly negative detuning, the efficiency of acoustic phonon scattering is indeed very low due to the energy difference between the initial and final states (Refs. 8–11).
[41] R. Guliamov, E. Lifshitz, E. Cohen, Arza Ron, and L. N. Pfeiffer, Phys. Rev. B **64**, 035314 (2001).
[42] M. Perrin, J. Bloch, A. Lemaître, and P. Senellart, Phys. Status Solidi C **2**, 759 (2005).
[43] C. Piermarocchi, F. Tassone, V. Savona, A. Quattropani, and P. Schwendimann, Phys. Rev. B **55**, 1333 (1997).